Trojan Horse Siderophore Conjugates Induce Pseudomonas aeruginosa Suicide and Qualify the TonB Protein as a Novel Antibiotic Target

Carsten Peukert, Veronique Gasser, Till Orth, Sarah Fritsch, Vincent Normant, Olivier Cunrath, Isabelle J Schalk, Mark Brönstrup

Trojan Horse siderophore conjugates induce *P. aeruginosa* suicide and qualify the TonB protein as a novel antibiotic target

Carsten Peukert[‡*], Véronique Gasser[# ~*], Till Orth[‡*], Sarah Fritsch[~], Vincent Normant[# ~], Olivier Cunrath[# ~], Isabelle Schalk[# ~], Mark Brönstrup[‡ § $]

‡ Department of Chemical Biology, Helmholtz Centre for Infection Research, Inhoffenstraße 7, 38124 Braunschweig

§ German Center for Infection Research (DZIF), Site Hannover-Braunschweig, 38124 Braunschweig, Germany

$ Center for Biomolecular Drug Research (BMWZ), Schneiderberg 38, 30167 Hannover

CNRS, University of Strasbourg, UMR7242, UMR7242, ESBS, Bld Sébastien Brant, F-67412 Illkirch, Strasbourg, France

~ University of Strasbourg, UMR7242, ESBS, Bld Sébastien Brant, F-67412 Illkirch, Strasbourg, France

* These authors contributed equally

Corresponding authors: Mark.Broenstrup@helmholtz-hzi.de and isabelle.schalk@unistra.fr

Abstract

Rising infection rates with multidrug-resistant bacterial pathogens such as *Pseudomonas* combined with a shallow antibiotic pipeline urgently call for antibiotics with novel modes of action. Herein, we identify the inner membrane protein TonB, motor of active uptake in Gram negative bacteria, as a novel target in antimicrobial therapy. The interaction of the TonB box, the periplasmic N-terminal domain of ferri-siderophore transporters, with the inner membrane protein TonB is crucial for the internalization of essential bacterial metabolites. Overexpression of a TonB box-containing peptide fragment in *P. aeruginosa* resulted in a growth repression, even in the presence of ferric heme as an iron source. The coupling of three TonB box peptides to synthetic DOTAM and MECAM siderophores with covalent or cleavable linkers of varying length and attachment sites yielded a panel of 24 conjugates in up to 32 synthetic steps. The transporters mediating iron uptake through these conjugates were identified by molecular approaches and transporter knockout mutants to be PfeA and PirA. The conjugates **11**, **13** and **17** repressed bacterial growth in *P. aeruginosa* strains with minimal inhibitory concentrations of 0.5, 4 and 0.1 μM, respectively. The study illustrates a variant of cellular suicide therapy where a transporter imports its own inhibitor; it also demonstrates that artificial siderophores are capable to import large cargo with molecular weights of up to 4 kDa, and suggests that TonB constitutes an attractive target for antimicrobial therapy.

Table of Content graphic

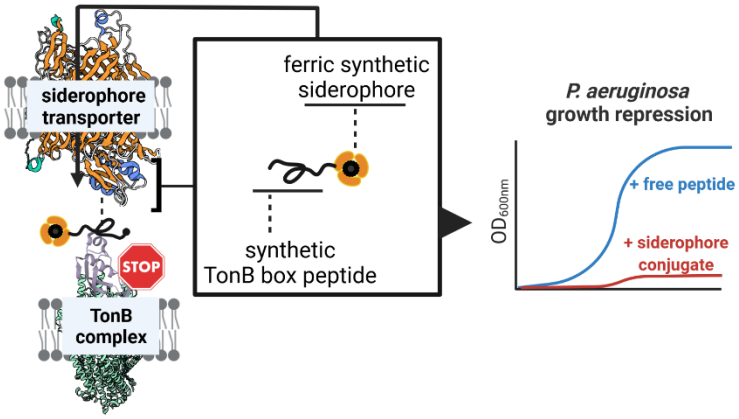

Introduction

Due to antibiotic overuse and a shallow antibiotic pipeline, nosocomial infections with multidrug-resistant (MDR) Gram-negative bacteria, e.g. *Pseudomonas aeruginosa* or *E. coli*, become increasingly difficult to treat.[1, 2, 3] Moreover, newly approved antimicrobials are largely derivatives of existing classes, while novel modes of action are scarce.[4, 5] 'Critical' pathogens on the WHO's priority list are all Gram-negative bacteria, mainly because they effectively prevent the accumulation of antibiotics by their double-layered cell membranes, that operate as a tight biological barrier.[6] The 'Trojan Horse' strategy outsmarts this hurdle by hijacking prokaryotic nutrient transport systems to increase the penetration of a variety of payloads (e.g. dyes, radioactive labels and antibiotics), to image and treat infections.[7, 8] A key nutrient of prokaryotes is iron, which fulfills numerous enzymatic und metabolic functions, enabling bacterial growth and pathogenicity. Bacteria evade iron limitation in the host organism through the import of heme and ferric iron. In the latter case this implies the synthesis and secretion of small, organic iron chelators, so-called siderophores (Greek for 'iron carriers').[9] After iron sequestration from host proteins, the ferric siderophore complexes are recaptured via specific outer membrane transporters called TonB-dependent transporters (TBDTs).[10] Ferric siderophores constitute cargo for TBDTs, but also other nutrients like heme, carbohydrates, nickel complexes and vitamin B_{12} are transported by TBDTs.[11] Interestingly, TBDTs have also been parasitized by bacteriophages and colicins to board the bacterial cell.[12] These transporters are unique to prokaryotes and present an unparalleled gateway to shuttle antibiotics inside bacterial pathogens.[13] This was demonstrated by the recently approved siderophore-cephalosporin antibiotic cefiderocol (Fetroja®).[14] The ability to transport even large cargo into bacteria is best illustrated by microcin MccE492, a natural product that consists of an 84 aa peptide chain attached via a sugar linkage to a triscatecholate chelator originating from enterobactin.[15] MccE492 exerts its antimicrobial effect at the cytoplasmic membrane after import. The application of natural siderophores as molecular targeting entities is in part hampered by their challenging synthetic access, their chemical lability as well as in some cases by their limited bacterial spectrum.[16, 17, 18, 19] Fortunately, much like piracy, prokaryotes seize so-called 'xenosiderophores' (siderophores produced by other organisms or even synthetic siderophore mimetics), to satisfy their iron demand.[20] Along those lines, we established enterobactin analogues based on synthetic DOTAM and MECAM scaffolds as robust, readily accessible and variable vectors for bacterial imaging and antibacterial therapy in Gram-negative and Gram-positive bacteria.[21, 22, 23]

TBDTs are composed of a 22 β-barrel inserted into the outer membrane, a plug domain that closes the channel formed by the barrel, and the TonB box.[10,24,25] The incoming ferric siderophore from the extracellular space binds to a specific site on the plug domain, promoting

the protein-protein interaction (PPI) between the TBDT's TonB box sequence and the TonB protein, that is anchored in the inner membrane and protrudes into the periplasm.[26] Located at the N-terminus of the TBDTs, the TonB box is a semiconserved stretch of five to seven amino acids that serves as a signature sequence for this transporter family. TonB is in complex with two other proteins ExbB and ExbD in the inner membrane (stoichiometry of 1:5:2 for TonB:ExbB:ExbD) and forms a molecular motor that uses the proton gradient of the inner membrane to convey energy to TBDTs, allowing the active transport of nutrients into the periplasmic space.[27] Alike a lock-and-key principle, the PPI between TonB and the TonB box of the TBDT promotes a conformational change in the transporter and permits the internalization of an iron-siderophore complex into the periplasm.[26] *P. aeruginosa* has three genes in its genome coding for TonB proteins (TonB1, TonB2 and TonB3), with solely TonB1 interacting with the TBDTs involved in iron or heme acquisition.[28] Moreover, the number of TonB proteins is very limited in relation to the different TBDTs in the outer membrane, implying a strong competition of TBDTs for TonB binding.[29] In previous studies, bacterial virulence, TonB-mediated colicin killing and φ80 phage infection could be reduced significantly by the treatment of *E. coli* with a species-specific, small TonB box consensus peptide (ETVIV), that was small enough to be internalized by polypeptide transporters.[30] However, an effect was only observed for high concentrations (>100 μM).

In this study, we aimed to explore the disruption of the TBDT-TonB interaction as a novel principle in antimicrobial therapy, with a proof-of-concept in the challenging pathogen *P. aeruginosa*. First, a conditional overexpression of a soluble TonB box peptide demonstrated the antimicrobial potential of this strategy. Secondly, a pharmacological approach was pursued by conjugating TonB box peptides of varying length to siderophore mimics, to enable accumulation at their target site inside the bacterial cell. Alike the natural microcins, an essential cellular machinery was preyed to import its own destroyer (Figure 1B).

RESULTS AND DISCUSSION

HasR TonB box peptide fragment overexpression induces growth reduction in *P. aeruginosa*

The Has system of *P. aeruginosa* extracts lipophilic heme from hemoglobin or hemopexin by a secreted hemophore to form a heme-hemophore complex, which is subsequently recognized by the TBDT HasR.[31, 32] Until recently, the TonB box location within the amino acid sequence of HasR remained unknown. We pinpointed the TonB box of *P. aeruginosa* HasR by pBLAST alignment with a HasR homolog from *Serratia marcescens*. The TonB box in *S. marcescens*

is located between the regulatory extension domain and the plug domain (Supplementary Figure S2).[33] Because these domains are highly conserved between species, we assumed that the TonB box of *P. aeruginosa* is located in the homologous region, and accordingly identified the peptide sequence [134]DLVQMSPSVI[141] as the putative TonB box in *P. aeruginosa*.

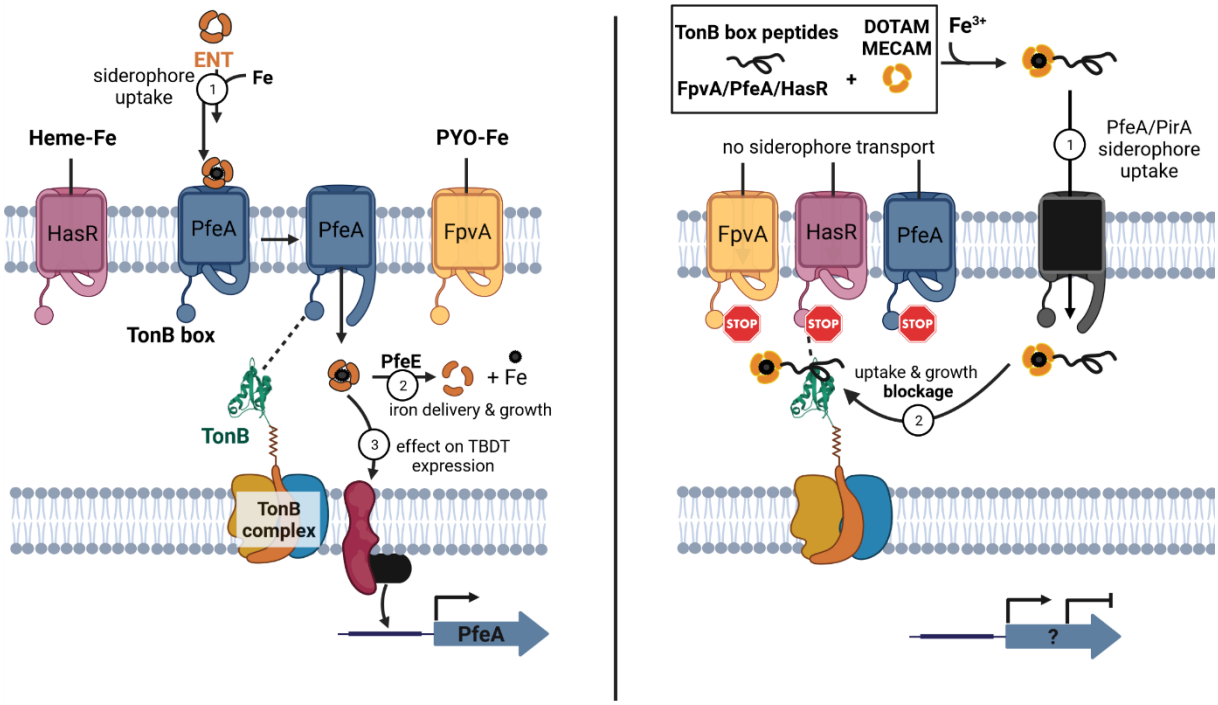

Figure 1: Iron delivery by enterobactin (ENT) (A) and envisioned suicide TonB siderophore strategy (B). (**A**) Iron chelators like heme, enterobactin (ENT) or pyoverdin (PYO) are recognized by their TonB-dependent transporters (TBDTs) HasR, PfeA and FpvA in *P. aeruginosa*. In the case of ferri-enterobactin, after internalization,the esterase PfeE hydrolyzes the siderophore to get release of iron. A fraction of ferri-enterobactin interacts with the two component system PfeS/PfeR regulating the transcription of *pfeA* and *pfeE* (**B**) Schematic depiction of the competitive inhibition of the TonB-TonB box interaction by peptide siderophore conjugates. Synthetic siderophores DOTAM or MECAM are coupled to TonB box peptides originating from the FpvA, PfeA, or HasR. The bacteria-specific vectors are transported into the periplasm and inhibit TonB function, thereby inhibiting uptake of additional iron or heme and consequently repressing bacterial growth.

A 172 amino acid fragment, containing the potential HasR TonB box, was cloned with a periplasmic localization sequence into a vector under the control of an arabinose promoter (araC/pbad, see SI) to yield the pMMB190-*araC-pbad-hasR*-His6 plasmid (Supplementary Figure S2). Transformed *P. aeruginosa* PAO1 bacteria were cultured in low iron (20 nM) casamino acid (CAA) medium with or without an induction with arabinose (1%) and with or

without 0.25 µM heme (Figure 2). As expected, addition of hemin stimulated *P. aeruginosa* growth in CAA medium, indicating that bacteria used heme as an iron source (red curve). Bacterial growth was reduced upon arabinose-induced peptide expression under both growth conditions, with and without heme. This suggests that the HasR TonB box peptide bound to the inner membrane TonB protein, subsequently interfered with TonB-dependent hemin internalization as well as probably with the pyoverdine and/or pyochelin-dependent iron uptake pathways used by the PAO1 strain when grown in the absence of hemin. Thus, less efficient iron sequestration resulted in a growth reduction. A similar study with overexpressing the N-terminal domain of FpvA (regulating and TonB box domains) showed an inhibition of ^{55}Fe uptake by pyoverdine (PYO).[34]

To examine the feasibility to construct a consensus sequence for TonB boxes within *Pseudomonas*, the sequence identified for HasR was compared with those for the transporter PfeA, that imports triscatecholate xenosiderophores like enterobactin (ENT), and for FpvA, that recognizes the endogenous siderophore PYO.[35, 36] However, the conservation between the curated sequences of FpvA (FPVA_PSEAE), PfeA (PFEA_PSEAE) and HasR (Q9HYJ7_PSEAE) retrieved from the UniProt database was low (score ≤0.3, black frame, Supplementary Figure S2).[37] In summary, the bioinformatics and microbiological data suggest that a TonB box peptide without transporter association can compete for TonB binding and prevent a vital PPI interaction, consequently inhibiting siderophore uptake. As a consensus sequence between the different TBDTs of *P. aeruginosa* could not be identified, the individual sequences were employed for follow-up experiments.

Design and synthesis of TonB box peptide DOTAM and MECAM siderophore conjugates

Next, we aimed to induce the growth inhibition, observed with the N-terminal HasR overexpression, through a pharmacological intervention with synthetic TonB box peptides. These were designed to compete for the TonB-TBDT protein-protein interaction. The lack of a consensus sequence of the employed TBDTs required the separate synthesis of the three corresponding peptides. Each peptide was afforded in a long and a short form, with either four to five (long) or one framing amino acid (short) around the TonB box (Figure 3B, 9-10 aa, bold). The peptides were too large for a passive permeation through porins or the lipid bilayer and thus required the conjugation to siderophore mimics as molecular 'Trojan Horses' to allow their penetration into the bacterial periplasm. Siderophores were attached to the N- or the C-terminus of the peptide by covalent or cleavable linkers. The artificial siderophores based on DOTAM (1,4,7,10-tetraazacyclododecane-1,4,7,10-tetraacetic amide) or MECAM (1,3,5-N,N',N″-tris-(2,3-dihydroxybenzoyl)-triaminomethylbenzene) scaffolds were equipped with an

alkyne handle for copper-catalyzed click chemistry according to established procedures (Figure 3C).[22, 23]

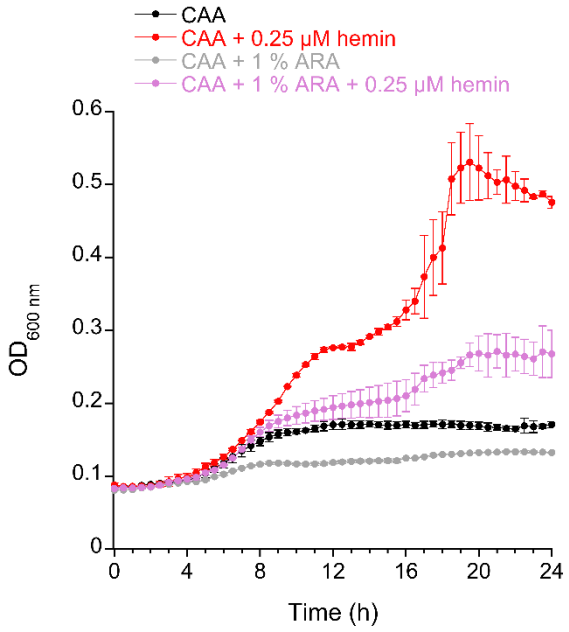

Figure 2: Growth of *P. aeruginosa* PAO1 transformed with pMMB190-araC-pbad-*hasR*-His_6 plasmid. The transformed bacteria were grown in CAA medium in the presence or not of 0.25 µM hemin and with or without arabinose (ARA, 1%) induction to induce the peptide expression. Bacterial growth is followed by monitoring optical density at 600 nm ($OD_{600\ nm}$). Errors bars were calculated from three independent biological replicates.

Starting from cyclen **43**, DOTAM siderophores **1** and **2** were prepared over four (38%) or five (30%) steps for the longest linear sequence, respectively (Scheme S1-S2). MECAM siderophores **3** and **4** were obtained from trisbromo-methylbenzene **47** over five (37%) or six steps (34%) in the longest linear sequence (Scheme S3). The peptides were synthetized on the solid phase using Fmoc-chemistry. More side product formation was observed for the HasR and FpvA peptides than for the PfeA peptides. This was attributed to the aspartic acid (D) and methionine (M) aa in their sequence, which are known to display i.e. succinamide formation[38] or oxidation to the sulfoxide under the reaction conditions.[39] In addition, also the unconjugated control peptides **5**-**10** were afforded (Schemes S5-S7, Table S1). For the synthesis of covalent conjugates, a N_3-PEG_7-CO_2H linker was attached at the C- or N-terminus of the peptide to permit the conjugation to **1**-**4** by copper-catalyzed azide alkyne additions (CuAAC). A C-terminal K(Dde) amino acid allowed the regioselective linker introduction after deprotection of the ε-amino function with hydrazine in THF/MeOH.[40] This yielded the DOTAM conjugates **11**-**21** and the MECAM conjugates **22**-**30** (Scheme S8-S10). In the case of **20** and **31**, the catechols were masked as acetylated prodrugs in order to avoid *in vivo* deactivation of the iron

chelating units by catechol-*O*-methyltransferases. Pyridyl disulfide chemistry was applied in the synthesis of the cleavable conjugates **21** and **32** that allowed an intracellular, reductive release of the peptide, thereby reducing steric hindrance of the siderophore (Scheme S10-11). The monocatechol-modified peptides **33** and **34** were constructed to reduce the overall molecular weight and still retain a TBDT-based internalization through a single chelator unit (Scheme S11). Taken together, 24 covalent or cleavable siderophore conjugates with a molecular weight of 3-4 kDa could be constructed in up to 32 synthetic steps.

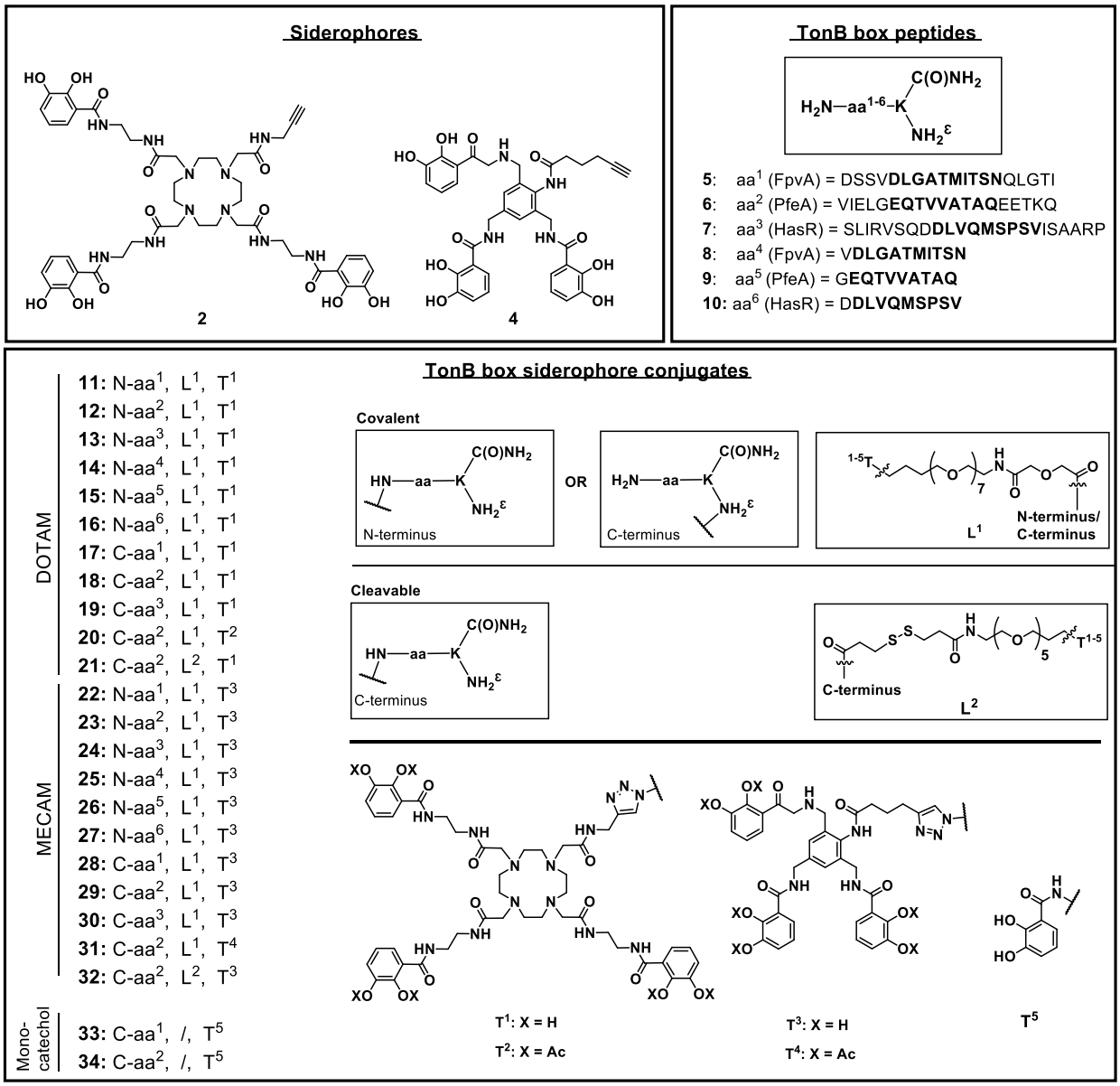

Figure 3: Structures of the DOTAM and MECAM siderophores **2** and **4**, TonB box peptides **5-10**, and siderophore-peptide conjugates **11-34**. The conjugates consist of a siderophore unit (T^x) that is linked via a covalent or a cleavable disulfide unit (L^x) to the N-terminus or the C-terminus of the peptide (aa^x).

All conjugates were characterized by ^{1}H-NMR and high resolution mass spectrometry, exemplary molecules also by ^{13}C-NMR, HSQC-NMR and tandem mass spectrometry (see the Supporting Information).

Peptide siderophore conjugates show antimicrobial effects in *P. aeruginosa*

The siderophores **2** and **4**, the peptides **5**-**10** and the siderophore conjugates **11-34** were evaluated for their antimicrobial activity in *P. aeruginosa* wild type and in siderophore-deficient *P. aeruginosa* mutant strains (*ΔpvdF ΔpchA*). The Δ*pvdF*Δ*pchA* mutant cannot biosynthesize its endogenous siderophores pyoverdine and pyochelin to access iron but probably uses low affinity iron uptake pathways like iron assimilation via citrate or an iron reduction process with uptake of Fe^{3+} by the FeoAB system. During an infection bacteria face an iron-starvation, as the host restrict iron access of the pathogens by nutritional immunity.[41] In order to test close to the *in vivo* infection conditions, all assays were conducted in iron-depleted CAA medium (20 nM iron).[42, 43] Along those lines, differential proteomics have shown that iron uptake pathways are solely expressed in *P. aeruginosa* cells under iron restricted conditions.[44] Compounds were first evaluated for the lowest compound concentration preventing visible bacterial growth in a standard minimal inhibitory concentration (MIC). In a second step, for a selection of compounds the ability to slow down bacterial growth was also evaluated.

MICs were determined after 24 and 48 h culture, as bacterial growth in iron-restricted conditions is slower than in an iron rich medium. While the positive control gentamicin exhibited an activity in the expected range, the free peptides **5-10** did not induce any growth inhibition (24 and 48 h). Also the free DOTAM and MECAM siderophores **2** and **4**, all MECAM conjugates as well as the monocatechols **33** and **34** remained inactive (Table 1). In contrast, several DOTAM conjugates inhibited bacterial growth. In particular, the long N-terminally linked conjugates **11** (FpvA)**, 12** (PfeA) and **13** (HasR) showed MICs of 0.5, 0.5 and 4 µM, respectively at 24 h. The most potent growth inhibition (MIC = 0.1 µM) was observed for **17**, that differs from **11** by its C-terminal (rather than N-terminal) linkage of the long FpvA-derived peptide. A moderate MIC of 8 µM was obtained for **21** that carries a cleavable linker to a long, PfeA-derived peptide. At 48 h, growth was recovered for conjugates **14**, **17** and **21**, but not for **11** and **12**. Possibly the peptide payloads exhibit an antimicrobial activity due an interaction with TonB, but over time either an adaptation of the bacteria or a degradation of the peptide payload by proteases takes place.[45] An attempt to increase the antimicrobial efficacy through a combination treatment of N- or C-terminal peptide siderophore conjugates did not result in a potency boost (data not shown). All compounds were inactive in the wildtype strain *P. aeruginosa* PAO1.

We reasoned that the high steric demand of the peptide payload might reduce the chelator's affinity for iron, thereby reducing uptake and antimicrobial activity. Therefore, the ability of the conjugates to sequester ferric iron was tested with chrome azurol S (CAS), whose color shifts from blue (iron bound state) to bright red upon iron decomplexation. A color change was not observed for the free peptides, while the siderophores **2** and **4** showed a clear color shift in the range from 300 to 800 nm, in line with previous reports (Supplementary Figure S3 and Table S9).[21, 22] Notably, all siderophore-peptide conjugates retained their ability to complex iron. From the experiments it becomes apparent that iron binding was possible, but the affinity may not be sufficient to compete with the wildtype siderophore PYO for ferric iron and to confer growth inhibition.

Table 1. MIC values in *P. aeruginosa ΔpvdFΔpchA* strain for siderophores **2** and **4**, peptides **5-10** and peptide-siderophore conjugates **11-34**.

Compound number	Description	MIC after 24 h	MIC after 48 h
-	Gentamicin	1	4
5	FpvA (l)	>64	>64
6	PfeA (l)	>64	>64
7	HasR (l)	>64	>64
8	FpvA (s)	>64	>64
9	PfeA (s)	>64	>64
10	HasR (s)	>64	>64
2	DOTAM	64	64
11	FpvA (l)-N-DOTAM	**0.5**	**1**
12	PfeA (l)-N-DOTAM	**0.5**	**1**
13	HasR (l)-N- DOTAM	**4**	**32**
14	FpvA (s)-N-DOTAM	32	>64
15	PfeA (s)-N-DOTAM	32	**32**
16	HasR (s)-N- DOTAM	>64	>64
17	FpvA (l)-C-DOTAM	**0.1**	>64
18	PfeA (l)-C-DOTAM	>64	>64
19	HasR (l)-C-DOTAM	>64	>64

20	PfeA (l)-C-DOTAM-OAc	>64	>64
21	PfeA (l)-DS-C-DOTAM	**8**	>64
4	MECAM	>64	>64
22	FpvA (l)-N-MECAM	>64	>64
23	PfeA (l)-N-MECAM	>64	>64
24	HasR (l)-N-MECAM	>64	>64
25	FpvA (s)-N-MECAM	>64	>64
26	PfeA (s)-N-MECAM	>64	>64
27	HasR (s)-N- MECAM	>64	>64
28	FpvA (l)-C-MECAM	>64	>64
29	PfeA (l)-C-MECAM	>64	>64
30	HasR (l)-C-MECAM	>64	>64
31	PfeA (l)-C-MECAM-OAc	>64	>64
32	PfeA (l)-DS-C-MECAM	>64	>64
33	FpvA-C-catechol	>64	>64
34	PfeA-C-catechol	>64	>64

MIC values were determined after 24 h and 48 h growth and are the mean of three independent experiments. (l) = long peptide, 20-24 aa, (s) = short peptide, 11-12 aa, C/N = C/N-terminal, DS = disulfide. Values are given in [μM], n = 3.

Peptide-siderophore conjugates enter the bacterial periplasm

Previously, we have employed ^{55}Fe uptake assays to demonstrate that MECAM or DOTAM have the ability to shuttle iron into bacteria through the TBDTs PfeA and PirA, or through PirA only, respectively.[46] Unfortunately, small precipitations of iron loaded conjugates we prohibited the execution of ^{55}Fe uptake assays with DOTAM and MECAM peptide conjugates with a sufficiently strong ^{55}Fe signal-to-noise ratio (data not shown). Consequently we exploited the property of ferri-siderophores to interact with the two component system PfeS/PfeR and induce *pfeA* transcription. Upon binding of periplasmic ferri-siderophore to the PfeS sensor at the inner membrane, the transcriptional regulator PfeR is released, upregulating the transcription of the *pfeA* gene.[47,48] Induction of *pfeA* transcription in the presence of the conjugates indicates the penetration of the compounds, since an interaction with PfeS can occur only in the periplasm. We have recently shown that unconjugated MECAM induced the transcription and expression

of *pfeA* by interacting with PfeS.[46] This induction was accompanied by a transcription repression of the genes involved in acquisition of iron by the siderophore pyochelin (PCH).[46]

The PYO and PCH-deficient Δ*pvdF*Δ*pchA* strain was grown over eight hours in iron-restricted CAA medium in the absence or presence of the peptides, free DOTAM and MECAM cores, and a selection of conjugates (**11**, **12**, **13**, **17**, **22** and **28**, each at 10 µM). The expression of the genes encoding *pfeA* (ferri-ENT TBDT),[36] *pirA* (ferri-ENT and ferri-catecholamines TBDT),[49, 50] *fpvA* (ferri-PYO TBDT),[24] and *fptA* (ferri-PCH TBDT)[51, 35, 52] was analyzed by differential quantitative real-time PCR (qRT-PCR) (Figure 4). Expectedly, the cores **2** and **4** showed a one to six (log2)fold induction of *pfeA* transcription in the PAO1 wildtype and *ΔpvdFΔpchA* mutant.[46] The free peptides **5-10** had no effect. For all tested MECAM and DOTAM conjugates, an induction of *pfeA* transcription was observed. This verifies their translocation into the periplasm and their interaction with the sensor PfeS at the inner membrane. The MECAM conjugates induced the transcription of *pfeA* with the same efficiency as the MECAM vector **4** alone. The DOTAM conjugates displayed an even stronger *pfeA* transcription induction than the free DOTAM vector **2**. None of the vectors or conjugates had a significant effect on *pirA* transcription. The transcription of *pirA*, such as of *pfeA,* is regulated by a two component system, namely PirS/PirR. Apparently the MECAM and DOTAM conjugates were able to bind to PfeS and induce a release of PfeR, but not to PirS.

All compounds, vectors and conjugates also induced a repression of *fptA* transcription. Interestingly, the highest fold changes concerning induction of *pfeA* and repression of *fptA* transcription were seen for the inactive MECAM conjugates, whilst the DOTAM conjugates generally had lower effects. This is probably due to a higher iron affinity of MECAM compared to DOTAM compounds. This adjustment of *pfeA* and *fptA* transcription indicates that the Δ*pvdF*Δ*pchA* strain adapted its TBDT expression for optimal iron acquisition via the conjugates in its surrounding. We also checked the ability of **11** to modulate the transcription of *pfeA*, *pirA*, *fpvA* and *fptA* in the PAO1 wildtype strain. However, their transcription was unaffected, possibly due to a higher efficacy of PYO and PCH to access iron than the larger **11**. In summary, both MECAM and DOTAM conjugates were able to cross the outer membrane of *P. aeruginosa*, because they induced a phenotypic adaptation of the bacteria (↑ *pfeA* transcription, ↓ *fptA* transcription). Consequently, we conclude that the antibiotic activity of the DOTAM conjugates was not due to iron sequestration by the compounds outside bacterial cells, but caused by internalized peptides, and probably an interaction of the peptides with TonB. All together these data indicate that the self-internalizing suicide Trojan horse mechanism is operational.

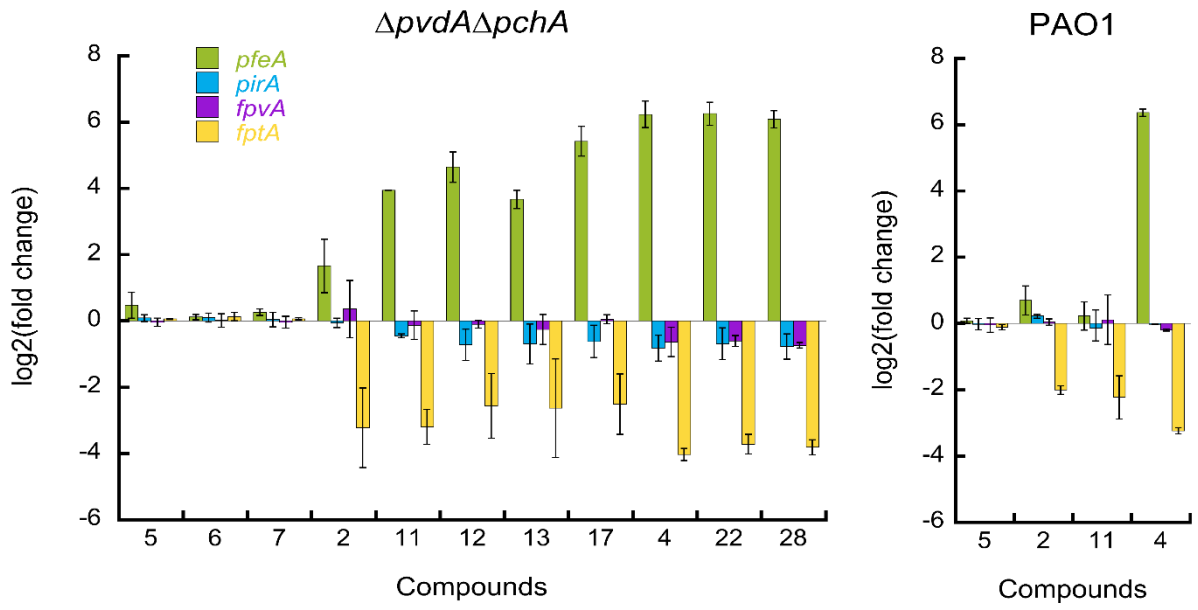

Figure 4. Modulation of TBDT gene expression by conjugates. *P. aeruginosa* Δ*pvdF*Δ*pchA* cells were grown for 8 h in the presence or absence of test compounds (10 µM). The transcription of *pfeA*, *pirA*, *fpvA* and *fptA* was followed by qRT-PCR.[42] *pfeA* encodes the ferri-ENT TBDT;[53,36] *pirA* the ferri-ENT and ferri-catecholamines TBDT[49, 50] *fpvA* the ferri-PYO TBDT[24] and *fptA* the ferri-PCH TBDT.[51, 52]

The transporters PfeA and PirA mediate the entry of conjugates in *P. aeruginosa* cells

Next, we aimed to elucidate the TBDT(s) involved in conjugate uptake. For this purpose, the growth of the *P. aeruginosa* Δ*pvdF*Δ*pchA* strain was compared to strains that carried additional TBDT deletions of (i) *pfeA*, (ii) *pirA* or (iii) *pfeA* and *pirA*. For compounds that do not exert antimicrobial activities, a growth reduction after TBDT knock-out proves that the missing siderophore transporter was crucial for the internalization of ferric chelates and thus permitted bacterial growth.[54, 46] The free peptides **5**-**7** exerted no effect (Figure 5). The growth of DOTAM-based conjugates was hardly impaired by missing PfeA, but a strong growth inhibition was observed for all mutants lacking PirA, indicating that all these compounds enter the cells through this TBDT. For MECAM-based conjugates the single deletion of PirA had no significant effect, whereas a lack of PfeA delayed growth slightly, in particular for the free MECAM **4** and the conjugate **29**. Interestingly, the dual knockout of *pfeA* and *pirA* genes led to a complete growth inhibition for all MECAM compounds, indicating that these compounds entered *P. aeruginosa* cells by both PfeA and PirA. This result also indicates that one receptor was able to rescue when the other receptor was absent or not functional. The data are in agreement with our recent finding that the MECAM core and a MECAM-ampicillin conjugate are transported into *P. aeruginosa* cells via PfeA and PirA, whereas DOTAM is solely internalized

via PirA.[46] We conclude that the transport mechanisms of the artificial siderophores were not altered by the conjugation of large peptidic cargo in the kilodalton range, and that the MECAM conjugates enter bacteria by either PfeA or PirA and the DOTAM conjugates by PirA.

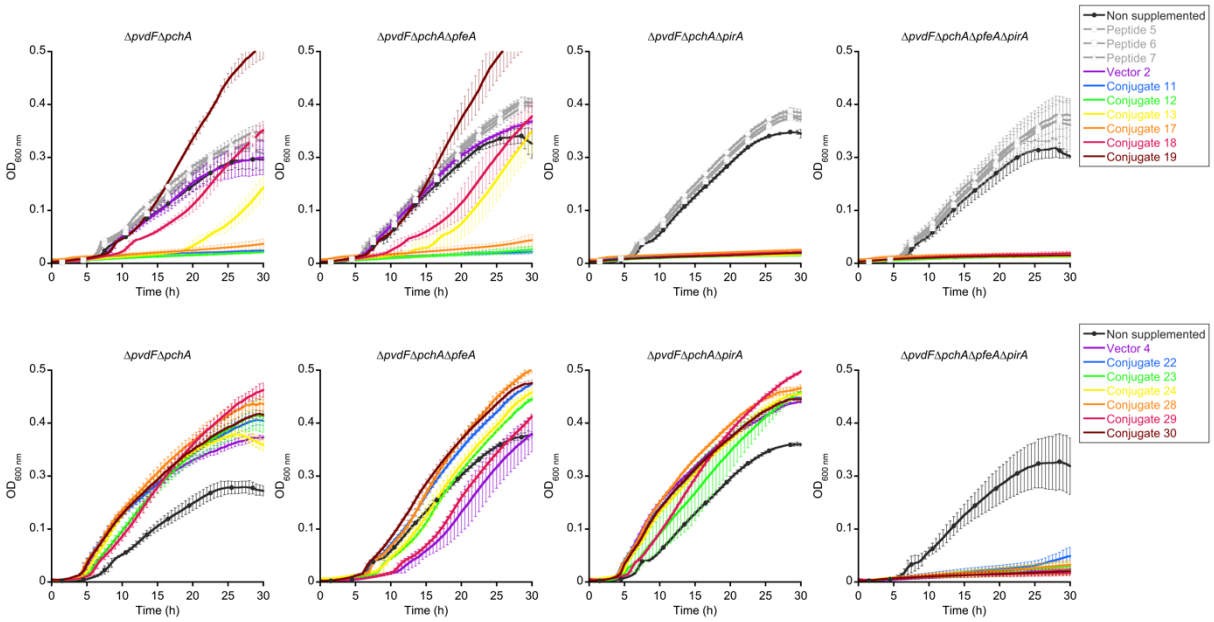

Figure 5. Growth kinetics of *P. aeruginosa pfeA* and *pirA* mutants in the presence of the conjugates. The PYO and PCH-deficient strain of *P. aeruginosa* (Δ*pvdF*Δ*pchA*) and its corresponding *pfeA* and *pirA* deletion mutants were used. Strains were grown in CAA medium in the absence or presence of 10 µM peptides **5**-**7**, DOTAM **2**, MECAM **4** or the conjugates **11**-**13**, **17**-**19**, **22**-**24** and **28**-**30**. Growth was followed by monitoring the optical density (OD) at 600 nm. Errors bars were calculated from three independent biological replicates.

CONCLUSION

In this study, we propose the disturbance of the interaction between TBDTs involved in the uptake of nutrient across the outer membrane of Gram negative bacteria and the TonB protein as a novel strategy to inhibit bacterial growth. A systematic attachment of siderophores to TonB box polypeptides from three TBDTS, coupled via cleavable or covalent linkers at the N- or C-terminus of the peptide to various of the targeting vectors (DOTAM and MECAM), yielded a diverse compound collection of two mono catechol peptides and 24 full siderophore conjugates. With molecular weights of up to 4 kDa, these are, to the best of our knowledge, among the largest synthetic siderophore conjugates. Their iron complexation capabilities were demonstrated by the CAS test. Growth recovery assays and their ability to induce the transcription of *pfeA* via the two component system PfeS/PfeR proved that all compounds were able to enter the periplasm of *P. aeruginosa*. All MECAM conjugates were internalized by PfeA

and PirA TBDTs, and DOTAM conjugates by PirA. A notable growth delay or inhibition, attributed to ferric siderophore internalization, was observed solely for DOTAM conjugates. The five conjugates **11**, **12**, **13**, **17** and **21** displayed antimicrobial activity in siderophore-deficient *P. aeruginosa* strains, and the most potent analogs **11** and **17** reached MICs of 0.5 and 0.1 µM, respectively. Based on the above data, we derive the following preliminary structure-activity relationships (SAR) (Supplementary Figure S4). Because all active compounds were based on the triscatecholate DOTAM vector, it was obviously better suited than MECAM. Conjugates with FpvA-originating peptides were more active compared to the equivalent congeners carrying sequences from PfeA and HasR. The active congeners had an N-terminal linkage rather than a C-terminal disulfide linker, and the longer peptides were superior to shorter ones.

Together, these results demonstrate the capability of MECAM and DOTAM to transport large cargo in the kilodalton range into bacteria. While first evidence in this direction has been obtained for the prototype natural product microcin MccE492, the data suggest that also artificial siderophores, coupled to synthetic linkers and peptides, can be employed. We realized the first siderophore 'Trojan Horse' antibiotics that target and disrupt a protein-protein interaction in the bacterial periplasm. Instead of satiating the pathogen's appetite for iron, the TonB box peptide payload competes with the TBDTs for TonB and thereby prevents the internalization of further ferric chelates. Thus, the study illustrates a variant of cellular suicide where a transporter imported its own inhibitor.

Perturbing the TonB-TBDT interaction is a novel principle to interfere with the pathogen's iron homeostasis and growth, yielding a decreased metabolism and fitness, and the conjugates described herein support the validity of the target. At this stage, structural information of the TonB box - TonB interaction at a molecular level would be beneficial to improve the understanding why only a subset of the conjugates was active. From here, it appears attractive to initiate a search for less complex small molecules that interfere with the PPI in future studies.

AUTHOR INFORMATION

Corresponding Author(s):

Mark Brönstrup - Department of Chemical Biology, Helmholtz Centre for Infection Research (HZI), German Center for Infection Research (DZIF), Site Hannover-Braunschweig, Inhoffenstraße 7, 38124 Braunschweig, Germany, Biomolecular Drug Research Center (BMWZ), 30167 Hannover. E-mail: Mark.Broenstrup@helmholtz-hzi.de ORCID: 0000-0002-8971-7045

Isabelle Schalk - CNRS, University of Strasbourg, UMR7242, ESBS, Bld Sébastien Brant, F-67412, Illkirch, Strasbourg, France

Further authors:

Carsten Peukert - Department of Chemical Biology, Helmholtz Centre for Infection Research (HZI), Inhoffenstraße 7, 38124 Braunschweig, Germany

Véronique Gasser - CNRS, University of Strasbourg, UMR7242, ESBS, Bld Sébastien Brant, F-67412, Illkirch, Strasbourg, France

Till Orth - Department of Chemical Biology, Helmholtz Centre for Infection Research (HZI), Inhoffenstraße 7, 38124 Braunschweig, Germany

Sarah Fritsch - University of Strasbourg, UMR7242, ESBS, Bld Sébastien Brant, F-67412 Illkirch, Strasbourg, France

Vincent Normant - CNRS, University of Strasbourg, UMR7242, ESBS, Bld Sébastien Brant, F-67412, Illkirch, Strasbourg, France

Olivier Cunrath - CNRS, University of Strasbourg, UMR7242, ESBS, Bld Sébastien Brant, F-67412, Illkirch, Strasbourg, France

FUNDING INFORMATION

The presented work was supported by a ‘Kekulé-Stipendium’ of the ‘Fonds der chemischen Industrie (VCI)’, as well as with a grant from the Joint Programming Initiative on Antimicrobial Resistance (JPI AMR, grant number: 01KI1825). We also acknowledge the Interdisciplinary Thematic Institute (ITI) InnoVec (Innovative Vectorization of Biomolecules, IdEx, ANR-10-IDEX-0002).

.

CONFLICT OF INTEREST

The authors declare no conflict of interest.

ACKNOWLEDGEMENTS

We thank Ulrike Beutling for the measurement of HRMS samples and Christel Kakoschke as well as Kirsten Harmrolfs for the measurement of NMR samples. We are thankful for helpful comments on the manuscript by Hazel Fuchs, Anna Vetter und Vadim Korotkov.

ABBREVIATIONS

TonB-dependent transporters, TBDT; proton-motive force, PMF; aa, amino acid; DOTAM, 1,4,7,10-tetraazacyclododecane-1,4,7,10-tetraacetic amide; MECAM, 1,3,5-N,N',N″-tris-(2,3-dihydroxybenzoyl)-triaminomethylbenzene, PPI, protein-protein interactions;

REFERENCES

1. Tacconelli, E.; Carrara, E.; Savoldi, A.; Harbarth, S.; Mendelson, M.; Monnet, D. L.; Pulcini, C.; Kahlmeter, G.; Kluytmans, J.; Carmeli, Y.; Ouellette, M.; Outterson, K.; Patel, J.; Cavaleri, M.; Cox, E. M.; Houchens, C. R.; Grayson, M. L.; Hansen, P.; Singh, N.; Theuretzbacher, U.; Magrini, N., Discovery, research, and development of new antibiotics: the WHO priority list of antibiotic-resistant bacteria and tuberculosis. *Lancet Infect. Dis.* **2018,** *18* (3), 318-327.

2. Murray, C. J. L.; Ikuta, K. S.; Sharara, F.; Swetschinski, L.; Robles Aguilar, G.; Gray, A.; Han, C.; Bisignano, C.; Rao, P.; Wool, E.; Johnson, S. C.; Browne, A. J.; Chipeta, M. G.; Fell, F.; Hackett, S.; Haines-Woodhouse, G.; Kashef Hamadani, B. H.; Kumaran, E. A. P.; McManigal, B.; Agarwal, R.; Akech, S.; Albertson, S.; Amuasi, J.; Andrews, J.; Aravkin, A.; Ashley, E.; Bailey, F.; Baker, S.; Basnyat, B.; Bekker, A.; Bender, R.; Bethou, A.; Bielicki, J.; Boonkasidecha, S.; Bukosia, J.; Carvalheiro, C.; Castañeda-Orjuela, C.; Chansamouth, V.; Chaurasia, S.; Chiurchiù, S.; Chowdhury, F.; Cook, A. J.; Cooper, B.; Cressey, T. R.; Criollo-Mora, E.; Cunningham, M.; Darboe, S.; Day, N. P. J.; De Luca, M.; Dokova, K.; Dramowski, A.; Dunachie, S. J.; Eckmanns, T.; Eibach, D.; Emami, A.; Feasey, N.; Fisher-Pearson, N.; Forrest, K.; Garrett, D.; Gastmeier, P.; Giref, A. Z.; Greer, R. C.; Gupta, V.; Haller, S.; Haselbeck, A.; Hay, S. I.; Holm, M.; Hopkins, S.; Iregbu, K. C.; Jacobs, J.; Jarovsky, D.; Javanmardi, F.; Khorana, M.; Kissoon, N.; Kobeissi, E.; Kostyanev, T.; Krapp, F.; Krumkamp, R.; Kumar, A.; Kyu, H. H.; Lim, C.; Limmathurotsakul, D.; Loftus, M. J.; Lunn, M.; Ma, J.; Mturi, N.; Munera-Huertas, T.; Musicha, P.; Mussi-Pinhata, M. M.; Nakamura, T.; Nanavati, R.; Nangia, S.; Newton, P.; Ngoun, C.; Novotney, A.; Nwakanma, D.; Obiero, C. W.; Olivas-Martinez, A.; Olliaro, P.; Ooko, E.; Ortiz-Brizuela, E.; Peleg, A. Y.; Perrone, C.; Plakkal, N.; Ponce-de-Leon, A.; Raad, M.; Ramdin, T.; Riddell, A.; Roberts, T.; Robotham, J. V.; Roca, A.; Rudd, K. E.; Russell, N.; Schnall, J.; Scott, J. A. G.; Shivamallappa, M.; Sifuentes-Osornio, J.; Steenkeste, N.; Stewardson, A. J.; Stoeva, T.; Tasak, N.; Thaiprakong, A.; Thwaites, G.; Turner, C.; Turner, P.; van Doorn, H. R.; Velaphi, S.; Vongpradith, A.; Vu, H.; Walsh, T.; Waner, S.; Wangrangsimakul, T.; Wozniak, T.; Zheng, P.; Sartorius, B.; Lopez, A. D.; Stergachis, A.; Moore, C.; Dolecek, C.; Naghavi, M., Global burden of bacterial antimicrobial resistance in 2019: a systematic analysis. *The Lancet* **2022,** *399* (10325), 629-655.

3. Thaden, J. T.; Park, L. P.; Maskarinec, S. A.; Ruffin, F.; Fowler, V. G.; Duin, D. v., Results from a 13-Year prospective cohort study show increased mortality associated with bloodstream infections caused by Pseudomonas aeruginosa compared to other bacteria. *Antimicrob. Agents Chemother.* **2017,** *61* (6), e02671-16.

4. Butler, M. S.; Gigante, V.; Sati, H.; Paulin, S.; Al-Sulaiman, L.; Rex, J. H.; Fernandes, P.; Arias, C. A.; Paul, M.; Thwaites, G. E.; Czaplewski, L.; Alm, R. A.; Lienhardt, C.; Spigelman, M.; Silver, L. L.; Ohmagari, N.; Kozlov, R.; Harbarth, S.; Beyer, P., Analysis of the clinical pipeline of treatments for drug resistant bacterial infections: despite progress, more action is needed. *Antimicrob. Agents Chemother.* **2022**, Aac0199121.

5. Theuretzbacher, U.; Gottwalt, S.; Beyer, P.; Butler, M.; Czaplewski, L.; Lienhardt, C.; Moja, L.; Paul, M.; Paulin, S.; Rex, J. H.; Silver, L. L.; Spigelman, M.; Thwaites, G. E.; Paccaud, J. P.; Harbarth, S., Analysis of the clinical antibacterial and antituberculosis pipeline. *Lancet Infect. Dis.* **2019,** *19* (2), e40-e50.

6. Breidenstein, E. B. M.; de la Fuente-Núñez, C.; Hancock, R. E. W., Pseudomonas aeruginosa: all roads lead to resistance. *Trends Microbiol.* **2011,** *19* (8), 419-426.

7. Klahn, P.; Bronstrup, M., Bifunctional antimicrobial conjugates and hybrid antimicrobials. *Nat. Prod. Rep.* **2017,** *34* (7), 832-885.

8. Miller, M. J.; Liu, R., Design and syntheses of new antibiotics inspired by nature's quest for iron in an oxidative climate. *Acc. Chem. Res.* **2021,** *54* (7), 1646-1661.

9. Hider, R. C.; Kong, X., Chemistry and biology of siderophores. *Nat. Prod. Rep.* **2010,** *27* (5), 637-657.

10. Schalk, I. J.; Mislin, G. L. A.; Brillet, K., Chapter two - structure, function and binding selectivity and steoselectivity of sderophore–ion oter memane tansporters. In *Curr. Top. Membr.*, Argüello, J. M.; Lutsenko, S., Eds. Academic Press: 2012; Vol. 69, pp 37-66.

11. Schauer, K.; Rodionov, D. A.; de Reuse, H., New substrates for TonB-dependent transport: do we only see the 'tip of the iceberg'? *Trends Biochem. Sci.* **2008,** *33* (7), 330-338.

12. Hickman, S. J.; Cooper, R. E. M.; Bellucci, L.; Paci, E.; Brockwell, D. J., Gating of TonB-dependent transporters by substrate-specific forced remodelling. *Nat. Comm.* **2017,** *8* (1), 14804.

13. Schalk, I. J.; Mislin, G. L. A., Bacterial Iron Uptake Pathways: Gates for the Import of Bactericide Compounds. *J. Med. Chem.* **2017,** *60* (11), 4573-4576.

14. Wu, J. Y.; Srinivas, P.; Pogue, J. M., Cefiderocol: A Novel Agent for the Management of Multidrug-Resistant Gram-Negative Organisms. *Infect. Dis. Ther.* **2020,** *9* (1), 17 – 40.

15. Duquesne, S.; Destoumieux-Garzón, D.; Peduzzi, J.; Rebuffat, S., Microcins, gene-encoded antibacterial peptides from enterobacteria. *Nat. Prod. Rep.* **2007,** *24* (4), 708-34.

16. Neumann, W.; Sassone-Corsi, M.; Raffatellu, M.; Nolan, E. M., Esterase-catalyzed siderophore hydrolysis activates an enterobactin-ciprofloxacin conjugate and confers targeted antibacterial activity. *J. Am. Chem. Soc.* **2018,** *140* (15), 5193 – 5201.

17. Raines, D. J.; Moroz, O. V.; Blagova, E. V.; Turkenburg, J. P.; Wilson, K. S.; Duhme-Klair, A. K., Bacteria in an intense competition for iron: Key component of the Campylobacter jejuni iron uptake system scavenges enterobactin hydrolysis product. *Proc. Natl. Acad. Sci.* **2016,** *113* (21), 5850-5855.

18. Mashiach, R.; Meijler, M. M., Total synthesis of pyoverdin D. *Org. Lett.* **2013,** *15* (7), 1702-1705.

19. Petrik, M.; Umlaufova, E.; Raclavsky, V.; Palyzova, A.; Havlicek, V.; Haas, H.; Novy, Z.; Dolezal, D.; Hajduch, M.; Decristoforo, C., Imaging of Pseudomonas aeruginosa infection with Ga-68 labelled pyoverdine for positron emission tomography. *Sci. Rep.* **2018,** *8* (1), 15698.

20. Perraud, Q.; Cantero, P.; Roche, B.; Gasser, V.; Normant, V. P.; Kuhn, L.; Hammann, P.; Mislin, G. L. A.; Ehret-Sabatier, L.; Schalk, I. J., Phenotypic Adaption of *Pseudomonas aeruginosa* by hacking siderophores produced by other microorganisms* *Mol. Cell. Proteomics* **2020,** *19* (4), 589-607.

21. Ferreira, K.; Hu, H.-Y.; Fetz, V.; Prochnow, H.; Rais, B.; Müller, P. P.; Brönstrup, M., Multivalent siderophore–DOTAM conjugates as theranostics for imaging and treatment of cacterial infections. *Angew. Chem. Int. Ed.* **2017,** *56* (28), 8272-8276.

22. Pinkert, L.; Lai, Y.-H.; Peukert, C.; Hotop, S.-K.; Karge, B.; Schulze, L. M.; Grunenberg, J.; Brönstrup, M., Antibiotic conjugates with an crtificial MECAM-Based siderophore are potent agents against Gram-positive and Gram-negative bacterial pathogens. *J. Med. Chem.* **2021,** *64* (20), 15440-15460.

23. Peukert, C.; Langer, L. N. B.; Wegener, S. M.; Tutov, A.; Bankstahl, J. P.; Karge, B.; Bengel, F. M.; Ross, T. L.; Brönstrup, M., Optimization of artificial siderophores as ^{68}Ga-complexed PET tracers for in vivo imaging of bacterial infections. *J. Med. Chem.* **2021,** *64* (16), 12359-12378.

24. Brillet, K.; Journet, L.; Célia, H.; Paulus, L.; Stahl, A.; Pattus, F.; Cobessi, D., A β Strand Lock Exchange for Signal Transduction in TonB-Dependent Transducers on the Basis of a Common Structural Motif. *Structure* **2007,** *15* (11), 1383-1391.

25. Llamas, M. A.; Mooij, M. J.; Sparrius, M.; Vandenbroucke-Grauls, C. M. J. E.; Ratledge, C.; Bitter, W., Characterization of five novel *Pseudomonas aeruginosa* cell-surface signalling systems. *Mol. Microbiol.* **2008,** *67* (2), 458-472.

26. Celia, H.; Noinaj, N.; Zakharov, S. D.; Bordignon, E.; Botos, I.; Santamaria, M.; Barnard, T. J.; Cramer, W. A.; Lloubes, R.; Buchanan, S. K., Structural insight into the role of the Ton complex in energy transduction. *Nature* **2016,** *538* (7623), 60-65.

27. Ratliff, A. C.; Buchanan, S. K.; Celia, H., Ton motor complexes. *Curr. Opin. Struct. Biol.* **2021,** *67*, 95-100.

28. DiRita, V. J.; Takase, H.; Nitanai, H.; Hoshino, K.; Otani, T., Requirement of the *Pseudomonas aeruginosa tonB* gene for high-affinity iron acquisition and infection. *Infect. Immun.* **2000,** *68* (8), 4498-4504.

29. Higgs, P. I.; Larsen, R. A.; Postle, K., Quantification of known components of the *Escherichia coli* TonB energy transduction system: TonB, ExbB, ExbD and FepA. *Mol. Microbiol.* **2002,** *44*.

30. Tuckman, M.; Osburne, M. S., In vivo inhibition of TonB-dependent processes by a TonB box consensus pentapeptide. *J. Bacteriol.* **1992,** *174* (1), 320-323.

31. Zygiel, E. M.; Obisesan, A. O.; Nelson, C. E.; Oglesby, A. G.; Nolan, E. M., Heme protects Pseudomonas aeruginosa and Staphylococcus aureus from calprotectin-induced iron starvation. *J. Biol. Chem.* **2021,** *296*, 100160.

32. Smith, A. D.; Modi, A. R.; Sun, S.; Dawson, J. H.; Wilks, A., Spectroscopic Determination of Distinct Heme Ligands in Outer-Membrane Receptors PhuR and HasR of Pseudomonas aeruginosa. *Biochemistry* **2015,** *54* (16), 2601-2612.

33. Létoffé, S.; Wecker, K.; Delepierre, M.; Delepelaire, P.; Wandersman, C., Activities of the *Serratia marcescens* heme receptor *HasR* and isolated plug and beta-barrel domains: The beta-barrel forms a heme-specific channel. *J. Bacteriol.* **2005,** *187* (13), 4637-45.

34. Nader, M.; Journet, L.; Meksem, A.; Guillon, L.; Schalk, I. J., Mechanism of ferripyoverdine uptake by *Pseudomonas aeruginosa* outer membrane transporter FpvA: No diffusion channel formed at any time during ferrisiderophore uptake. *Biochemistry* **2011,** *50* (13), 2530-2540.

35. Cobessi, D.; Celia, H.; Folschweiller, N.; Schalk, I. J.; Abdallah, M. A.; Pattus, F., The crystal structure of the pyoverdine outer membrane receptor FpvA from Pseudomonas aeruginosa at 3.6Å resolution. *J. Mol. Biol.* **2005,** *347* (1), 121-134.

36. Moynié, L.; Milenkovic, S.; Mislin, G. L. A.; Gasser, V.; Malloci, G.; Baco, E.; McCaughan, R. P.; Page, M. G. P.; Schalk, I. J.; Ceccarelli, M.; Naismith, J. H., The complex of ferric-enterobactin with its transporter from Pseudomonas aeruginosa suggests a two-site model. *Nat. Comm.* **2019,** *10* (1), 3673.

37. Zimmermann, L.; Stephens, A.; Nam, S.-Z.; Rau, D.; Kübler, J.; Lozajic, M.; Gabler, F.; Söding, J.; Lupas, A. N.; Alva, V., A completely reimplemented MPI bioinformatics toolkit with a new HHpred server at its core. *J. Mol. Biol.* **2018,** *430* (15), 2237-2243.

38. Capasso, S.; Mazzarella, L.; Sica, F.; Zagari, A.; Salvadori, S., Spontaneous cyclization of the aspartic acid side chain to the succinimide derivative. *J. Chem. Soc. Chem. Comm.* **1992,** (12), 919-921.

39. Schilter, D., Thiol oxidation: A slippery slope. *Nat. Rev. Chem.* **2017,** *1* (2), 0013.

40. Díaz-Mochón, J. J.; Bialy, L.; Bradley, M., Full Orthogonality between Dde and Fmoc: The direct Synthesis of PNA−peptide conjugates. *Org. Lett.* **2004,** *6* (7), 1127-1129.

41. Cassat, James E.; Skaar, Eric P., Iron in infection and immunity. *Cell Host & Microbe* **2013,** *13* (5), 509-519.

42. Gasser, V.; Baco, E.; Cunrath, O.; August, P. S.; Perraud, Q.; Zill, N.; Schleberger, C.; Schmidt, A.; Paulen, A.; Bumann, D.; Mislin, G. L. A.; Schalk, I. J., Catechol siderophores repress the pyochelin pathway and activate the enterobactin pathway in Pseudomonas aeruginosa: an opportunity for siderophore–antibiotic conjugates development. *Environ. Microbiol.* **2016,** *18* (3), 819-832.

43. Cunrath, O.; Geoffroy, V. A.; Schalk, I. J., Metallome of *Pseudomonas aeruginosa*: A role for siderophores. *Environ. Microbiol.* **2016,** *18* (10), 3258-3267.

44. Perraud, Q.; Cantero, P.; Munier, M.; Hoegy, F.; Zill, N.; Gasser, V.; Mislin, G. L. A.; Ehret-Sabatier, L.; Schalk, I. J., Phenotypic adaptation of *Pseudomonas aeruginosa* in the presence of siderophore-antibiotic conjugates during epithelial cell infection. *Microorganisms* **2020,** *8* (11), 1820.

45. Culp, E.; Wright, G. D., Bacterial proteases, untapped antimicrobial drug targets. *J. Antibiot.* **2017,** *70* (4), 366-377.

46. Fritsch, S.; Gasser, V.; Peukert, C.; Pinkert, L.; Kuhn, L.; Perraud, Q.; Normant, V.; Brönstrup, M.; Schalk, I., Uptake mechanisms and regulatory responses to MECAM- and DOTAM-based artificial siderophores and their antibiotic conjugates in Pseudomonas aeruginosa. *ACS Infect. Dis.* **2022**.

47. Dean, C. R.; Neshat, S.; Poole, K., PfeR, an enterobactin-responsive activator of ferric enterobactin receptor gene expression in *Pseudomonas aeruginosa*. *J. Bacteriol.* **1996,** *178* (18), 5361-5369.

48. Gasser, V.; Kuhn, L.; Hubert, T.; Aussel, L.; Hammann, P.; Schalk, I. J., The esterase PfeE, the achilles' Hheel in the battle for Iron between *Pseudomonas aeruginosa* and *Escherichia coli*. *Int. J. Mol. Sci.* **2021,** *22* (6), 2814.

49. Ghysels, B.; Ochsner, U.; Möllman, U.; Heinisch, L.; Vasil, M.; Cornelis, P.; Matthijs, S., The Pseudomonas aeruginosa *pirA* gene encodes a second receptor for ferrienterobactin and synthetic catecholate analogues. *FEMS Microbiol. Lett.* **2005,** *246* (2), 167-174.

50. Perraud, Q.; Kuhn, L.; Fritsch, S.; Graulier, G.; Gasser, V.; Normant, V.; Hammann, P.; Schalk, I. J., Opportunistic use of catecholamine neurotransmitters as siderophores to access iron by *Pseudomonas aeruginosa*. *Environ. Microbiol.* **2022,** *24* (2), 878-893.

51. Ankenbauer, R. G.; Quan, H. N., FptA, the Fe(III)-pyochelin receptor of *Pseudomonas aeruginosa*: A phenolate siderophore receptor homologous to hydroxamate siderophore receptors. *J. Bacteriol.* **1994,** *176* (2), 307-319.

52. Cobessi, D.; Celia, H.; Pattus, F., Crystal structure at high resolution of ferric-pyochelin and its membrane receptor FptA from *Pseudomonas aeruginosa*. *J. Molec. Biol.* **2005,** *352* (4), 893-904.

53. Dean, C. R.; Poole, K., Cloning and characterization of the ferric enterobactin receptor gene (pfeA) of *Pseudomonas aeruginosa*. *J. Bacteriol.* **1993,** *175* (2), 317-324.

54. Perraud, Q.; Cantero, P.; Roche, B.; Gasser, V.; Normant, V. P.; Kuhn, L.; Hammann, P.; Mislin, G. L. A.; Ehret-Sabatier, L.; Schalk, I. J., Phenotypic adaption of *Pseudomonas aeruginosa* by hacking siderophores produced by other microorganisms*. *Mol. Cell. Proteom.* **2020,** *19* (4), 589-607.